AD-A110 379 NAVAL SURFACE WEAPONS CENTER SILVER SPRING MD F/6 12/1
ALGORITHMS FOR THE ESTIMATION OF TIME DELAY AND TIME DELAY RATE--ETC(U)
AUG 81 A K CHRYSOSTOMOU, R S HEBBERT
UNCLASSIFIED NSWC-TR-81-303 NL

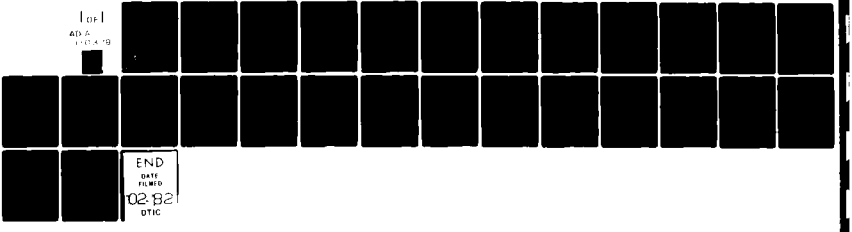

END
DATE FILMED
02-82
DTIC

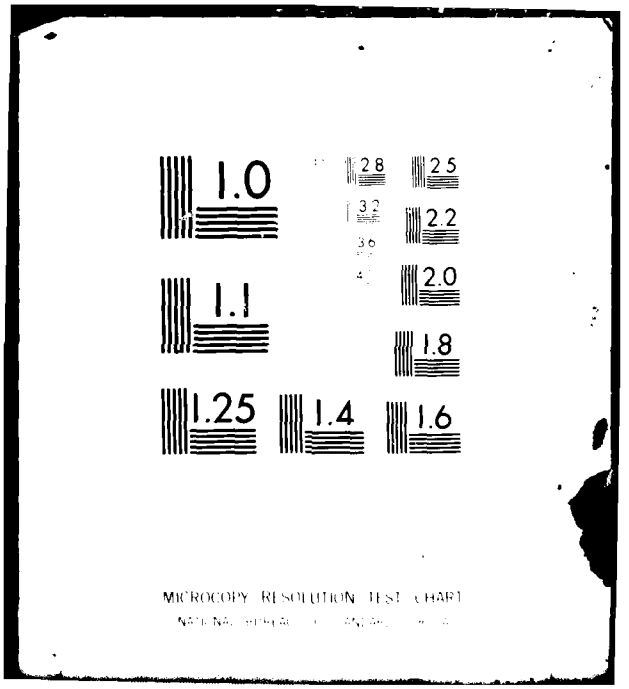
1.0
2.8
2.5
3.2
2.2
3.6
4.0
2.0
1.1
1.8
1.25
1.4
1.6
MICROCOPY RESOLUTION TEST CHART

NSWC TR 81-303

LEVEL II

AD A110379

ALGORITHMS FOR THE ESTIMATION OF TIME DELAY AND TIME DELAY RATE

BY A. K. CHRYSOSTOMOU AND R. S. HEBBERT

UNDERWATER SYSTEMS DEPARTMENT

1 AUGUST 1981

NAVAL SURFACE WEAPONS CENTER

Dahlgren, Virginia 22448 • Silver Spring, Maryland 20910

82

UNCLASSIFIED

SECURITY CLASSIFICATION OF THIS PAGE (When Data Entered)

REPORT DOCUMENTATION PAGE	READ INSTRUCTIONS BEFORE COMPLETING FORM
1. REPORT NUMBER: NSWC TR 81-303	2. GOVT ACCESSION NO.: AD-A110 329
3. RECIPIENT'S CATALOG NUMBER	
4. TITLE (and Subtitle): ALGORITHMS FOR THE ESTIMATION OF TIME DELAY AND TIME DELAY RATE	5. TYPE OF REPORT & PERIOD COVERED: Final
	6. PERFORMING ORG. REPORT NUMBER
7. AUTHOR(s): A. K. Chrysostomou R. S. Hebbert	8. CONTRACT OR GRANT NUMBER(s)
9. PERFORMING ORGANIZATION NAME AND ADDRESS: Naval Surface Weapons Center (CODE U22) White Oak, Silver Spring, Maryland 20910	10. PROGRAM ELEMENT, PROJECT, TASK AREA & WORK UNIT NUMBERS: 64261N, W1102-AS, 134DC
11. CONTROLLING OFFICE NAME AND ADDRESS: Manager, Antisubmarine Warfare Systems Project Office, Department of the Navy Washington, D. C. 20360 (PM-4)	12. REPORT DATE: 1 August 1981 13. NUMBER OF PAGES: 30
14. MONITORING AGENCY NAME & ADDRESS(if different from Controlling Office)	15. SECURITY CLASS. (of this report): UNCLASSIFIED 15a. DECLASSIFICATION/DOWNGRADING SCHEDULE

16. DISTRIBUTION STATEMENT (of this Report)

Approved for public release; distribution unlimited.

17. DISTRIBUTION STATEMENT (of the abstract entered in Block 20, if different from Report)

18. SUPPLEMENTARY NOTES

19. KEY WORDS (Continue on reverse side if necessary and identify by block number)

Cross correlation
Time delay estimation
Doppler compensation
Time delay rate

20. ABSTRACT (Continue on reverse side if necessary and identify by block number)

The purpose of this report is to present two generalized cross-correlation algorithms for the estimation of the time delay and time delay rate parameters. The implementation of these algorithms is done on a CSPI MAP-300 array processor and a PDP 11/34 as the host computer. The performance of the algorithms is evaluated in real time with simulated and real data.

DD FORM 1 JAN 73 1473 EDITION OF 1 NOV 65 IS OBSOLETE
S/N 0102-LF-014-6601

UNCLASSIFIED

SECURITY CLASSIFICATION OF THIS PAGE (When Data Entered)

FOREWORD

The estimation of the time delay between signals arriving at two spatially separated sensors is investigated, for the purpose of target localization. The real data were obtained during a sea test.

F. B. Sanchez

F. B. SANCHEZ
By direction

CONTENTS

ILLUSTRATIONS

INTRODUCTION

This report examines at first the estimation of time delay $\tau(t)$ and secondly the estimation of time delay and delay rate $\dot{\tau}(t)$ (doppler shift), between signals received at two spatially separated sensors in the presence of uncorrelated noise. The mathematical models for both estimation procedures assume stationarity for the characteristics of signal and noise for a finite observation time T. It is also assumed that the spectral characteristics of the signal are known.

ONE DIMENSIONAL SEARCH FOR THE ESTIMATION OF THE TIME DELAY $\tau(t)$

FORMULATION AND ANALYSIS.

A signal s(t) emanating from an acoustic source and received, in the presence of noise, at two spatially separated sensors can be mathematically modeled, as shown in Figure 1, as follows:

$$x_1(t) = s(t) + n_1(t) \tag{1-1}$$

$$x_2(t) = s(t-\tau(t)) + n_2(t) \tag{1-2}$$

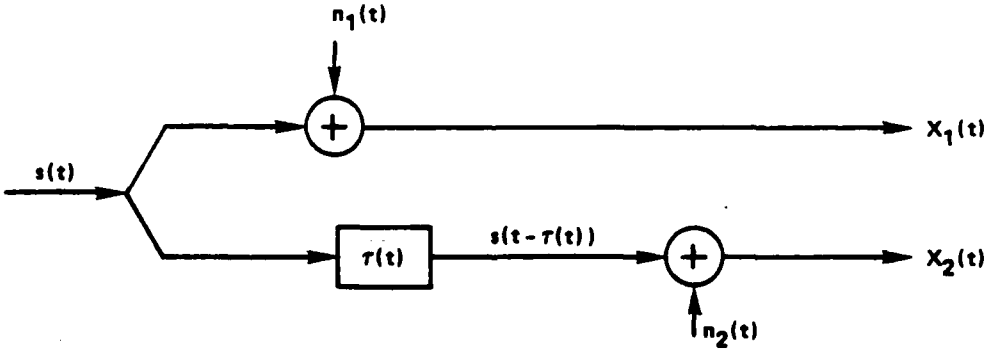

FIGURE 1 SIGNAL DELAYED AND CORRUPTED BY NOISE, RECEIVED AT THE TWO SENSORS

It is assumed that s(t), $n_1(t)$, $n_2(t)$ are jointly stationary random processes, and the signal s(t) is uncorrelated with noise $n_1(t)$ and $n_2(t)$, i.e.,

$$E\{s(t)n_1^*(t)\} = E\{s(t)n_2^*(t)\} = 0,$$

where E denotes expectation and * complex conjucate. We also assume that we have real random processes and furthermore,

$$E\{s(t)s^*(t)\} = Q,\ E\{n_i(t)n_j^*(t)\} = R\delta_{ij}, i,\ j = 1,2$$

The time delay τ is the parameter to be estimated by $\hat{\tau}$. One method of such estimation ([1]) is to maximize the crosscorrelation function.

$$R_{x_1,\ x_2}(\tau) = E\{x_1(t)x_2^*(t-\tau)\} \tag{1-3}$$

The argument $\tau = \hat{\tau}$ that achieves the above maximum is the desired time delay estimate.

For the given model we have, under the assumptions:

$$R_{x_1,\ x_2}(\hat{\tau}) = R_{s,s}(\tau-\hat{\tau}) + R_{n_1,\ n_2}(\hat{\tau}) \tag{1-4}$$

The Fourier transform of (1-4) gives the cross-spectrum:

$$S_{x_1,x_2}(f) = S_{s,s}(f)e^{-2\pi jf\tau} + S_{n_1,n_2}(f) \tag{1-5}$$

Since

$$R_{n_1,n_2}(\tau) = 0, \text{ then } S_{n_1,\ n_2}(f) = 0 \tag{1-6}$$

From (1-6), equation (1-5) is equivalent, in the time domain, to:

$$R_{x_1,x_2}(\hat{\tau}) = R_{s,s}(\hat{\tau}) \bullet \delta(\hat{\tau}-\tau) \tag{1-7}$$

where $\bullet$ denotes convolution.

Equation (1-7) says that the delta function has been "smeared" by the signal. If the signal s(t) is white noise, only then the delta function is not spread and the $\hat{\tau}$ is the position of the delta function. For this special case, see Figure 7. In this figure, the white noise signal received at one sensor relative to the other, is delayed by

$$\tau = 0,\ -1/8,\ -1/4 \text{ seconds.}$$

Each correlogram is averaged for 4 seconds. During the first 24 seconds we have infinite signal to noise ratio, while for the remaining time we have S/N ratio = -15 dB. Different delay rates, positive and negative, are also illustrated.

IMPLEMENTATION.

The above time delay estimation procedure was implemented in the MAP-300 array processor and the PDP 11/34 as the host computer. As a continuation of the block diagram in Figure 1, consider the block diagram of Figure 2, describing the algorithm.

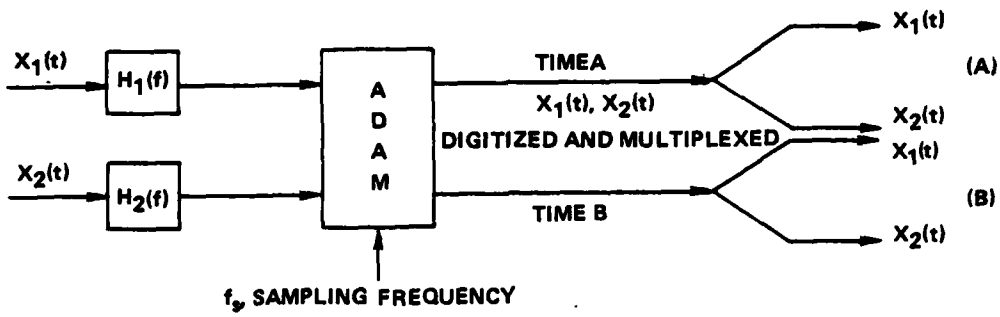

FIGURE 2 BLOCK DIAGRAM OF THE TIME DELAY ESTIMATOR

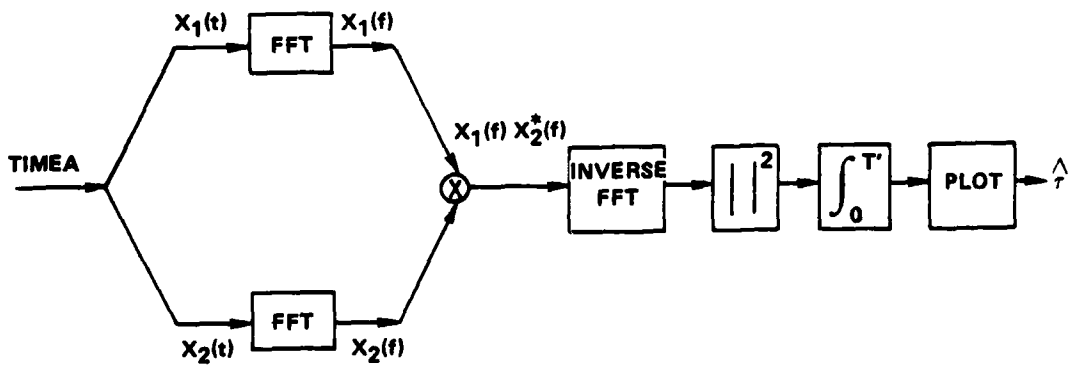

FIGURE 3 BLOCK DIAGRAM OF THE TIME DELAY ESTIMATOR

From Figure 2, the time sequences $x_1(t)$, $x_2(t)$ go through the low-pass filters $H_1(f)$, $H_2(f)$. The maximum signal frequency, f_{max}, allowed through these filters is such that $f_s \geq 2.5 f_{max}$, where f_s is the sampling frequency. Once this is done, the filtered sequences $x_1(t)$, $x_2(t)$ enter the ADAM (Analog Digital Acquisition Module) where they are sampled at the rate fs, and multiplexed. This process is controlled by the software. Once sampled, one of the double buffers labeled TIMEA, and containing both digitized sequences $x_1(t)$, $x_2(t)$, is processed by the MAP-300, while the other double buffer TIMEB is being filled with the new digitized data. This guarantees that no data is lost during the processing and furthermore, it guarantees parallel processing between the ADAM, the MAP-300 and the host computer.

Figure 3 shows the demultiplexing of the time sequences, which are then FFT'd, cross-multiplied after one has been conjucated and the cross product inverse FFT'd. From the resulting complex time sequence, we obtain a real time sequence by taking the power in each of the cells of this complex sequence. The resulting real time sequence is the correlogram (Eq. (1-7)), which is averaged for T' seconds. The averaged correlograms are then plotted on the Tektronix 4014 by using Fortran calls from the host computer.

It is of importance to note that all of the above procedure depicted in Figure 3 is done in the MAP 300 in such a way as to achieve maximum speed during the real time processing of the data. It is also important to note the sychronization (parallel processing) between the MAP-300 and the host computer. The time during which it takes the host to plot the $(k-1)^{th}$ correlogram, the MAP-300 is processing the data obtained from the double buffer TIMEB (part (B) of Figure 2). So by the time the plotting of the $(k-1)^{th}$ correlogram is completed, the k^{th} correlogram is available to the host for plotting.

The duration T, of the FFT shown in Figure 3 is $T = N/fs$, where N is the number of points in each of the channels $x_1(t)$, $x_2(t)$, and fs is the sampling frequency. A typical sampling duration T is $T = 1$ sec. This provides the capability to search for $\hat{\tau}$ in a delay window from -1/2 to +1/2 seconds. Based on the distance between the sensors the delay window can vary by appropriately varying N or f_s or both. Also, the number of seconds for the post-integration of the correlogram is a variable. If $T' = 4$ sec and $T = 1$ sec (duration of a time cut) and if we have 10 minutes of data to process (600 time cuts), the number of correlograms plotted is $N_1 = 600/T' = 150$.

Following a spectral analysis of the signal, based on its spectral characteristics, we may want to process only a spectral window around some center frequency f_o. The outlined algorithm is capable of doing this, by extracting any spectral window for every channel and searching for $\hat{\tau}$, based on the energy of the signal inside this spectral band.

The algorithm described above is successful in estimating the time delay between signals received at sensors closely spaced together and between signals from a nonmaneuvering target moving at a relatively low speed.

---

[1]Knapp C. H. and Carter G. C., "The Generalized Correlation Method for Estimation of Time Delay," IEEE Trans. Acous., Speech, and Signal Proc., Vol. ASSP-24, No. 4, pp. 320-327, Aug 1976.

It is known that the received frequency at a sensor due to the relative motion between the target and sensor is given by

$$f = f_o \left(1 - \frac{v\cos\phi}{c}\right) \tag{1-8}$$

where:

f: received frequency

f_o: radiated frequency

v: target velocity

c: speed of underwater sound

ϕ: angle between target velocity vector and the line between sensor and target.

Equation (1-8) shows that it is necessary to compensate for the high doppler shift arising from maneuvering targets or targets moving at high speed. The analysis and algorithm that follow consist of a two dimensional search in which in addition to the estimation of time delay $\tau(t)$ an estimate of the time delay rate $\dot{\tau}(t)$ is obtained to accommodate for the cases mentioned above.

TWO DIMENSIONAL SEARCH FOR THE ESTIMATION OF THE TIME DELAY $\tau(t)$ AND TIME DELAY RATE $\dot{\tau}(t)$

FORMULATION AND ANALYSIS.

As in Part 1 of this report, let $s(t)$ be the radiated signal and let $n_1(t)$, $n_2(t)$ the noise received at the two sensors. Under the same assumptions we have

$$x_1(t) = s(t) + n_1(t) \tag{2-1}$$

$$x_2(t) = s(t - \tau + \alpha t) + n_2(t) \tag{2-2}$$

where τ and α are the delay and delay rate respectively to be estimated. Furthermore, let the time series $x_1(t)$, $x_2(t)$ be heterodyned and appropriately filtered with weights $w(t)$. The block representation of this procedure is shown in Figure 4.

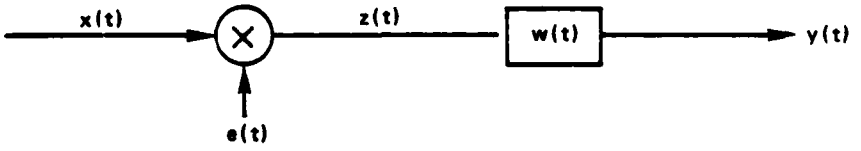

FIGURE 4 HETERODYNE AND LOW-PASS OF THE TIME SEQUENCE

We have $z(t) = x(t)\, e(t)$

and $$y(t) = z(t) \circledast w(t) = x(t)e(t) \circledast w(t) \tag{2-3}$$

where $e(t) = e^{-i\omega_h t}$

$$w(t) = \frac{1}{2}\left(1-\cos\frac{2\pi t}{T}\right),\ 0 \le t \le T \tag{2-4}$$

the Hanning weights.

For each time series $x_1(t)$, $x_2(t)$ we have:

$$y_1(t) = \int_{-\infty}^{\infty} x_1(s_1 + t)e^{-i\omega_h(s_1 + t)}w(s_1)ds_1 \tag{2-5}$$

$$y_2(t) = \int_{-\infty} x_2(s_2 + t)e^{-i\omega_h(s_2 + t)}w(s_2)ds_2 \tag{2-6}$$

$$\text{But } x_2(t) = x_1(t-\tau_o + \alpha t) = x_1((1+\alpha)t-\tau_o) \tag{2-7}$$

$$\text{Also let } E\left\{x_1(t)x_1^*(t')\right\} = R(t-t') \tag{2-8}$$

Then the crosscorrelation function of the output series

$y_1(t)$, $y_2(t)$ is

$$R_{y_1,y_2}(\tau) = E\{y_1(t-\tau)y_2^*(t)\} =$$

$$= \int_{-\infty}^{\infty}\int_{-\infty}^{\infty} E\{x_1(s_1+t-\tau)x_2^*(s_2+t)\}e^{-i\omega_h(s_1-s_2-\tau)}w(s_1)w(s_2)ds_1ds_2$$
$$= \int_{-\infty}^{\infty}\int_{-\infty}^{\infty} E\{x_1(s_1+t-\tau)x_1^*((1+\alpha)(s_2+t)-\tau_o)\}e^{-i\omega_h(s_1-s_2-\tau)}w(s_1)w(s_2)ds_1ds_2$$
$$= \int_{-\infty}^{\infty}\int_{-\infty}^{\infty} R[(s_1+t-\tau)-((1+\alpha)(s_2+t)-\tau_o)]e^{-i\omega_h(s_1-s_2-\tau)}w(s_1)w(s_2)ds_1ds_2 \tag{2-9}$$

If the signal is white noise then

$$R_{x_1,x_1} = E\{x_1(t)x_1^*(t')\} = R(t-t') = \delta(t-t') \tag{2-10}$$

and Eq. (2-9) becomes for

$$s_1 = (1+\alpha)s_2 + (\tau-\tau_o) + \alpha t \text{ and } s_2 = s, \tag{2-11}$$

$$R_{y_1,y_2}(\tau) = \int_{-\infty}^{\infty} e^{-i\omega_h(\alpha s+\alpha t-\tau_o)}w(s)w((1+\alpha)s+(\tau-\tau_o+\alpha t))ds \tag{2-12}$$

We can write $\tau-\tau_o+\alpha t$ as

$\tau-\tau_o+\alpha t = \epsilon_1 + \epsilon_2 t$ where

ϵ_1 is the error in estimating τ_o(the time delay)
and ϵ_2 is the error in estimating α (the time delay rate)

IMPLEMENTATION.

The implementation of equations (2-5) and (2-6) in the MAP-300 was done by using the DCVM (Discrete Convolution Multiply) and CXMUL (Complex Multiply) calls. If we let T be the sampling time, f_h the heterodyne frequency, f_s the sampling frequency and N the number of points in the time series, then the "select" function e(t) in the discrete case becomes:

$$e_k = e^{-i\omega_h t_k} = e^{-2\pi i f_h kT/N} = e^{-2\pi i f_h (T/N)k} = e^{-2\pi i (\frac{f_h}{f_s})k} \qquad (2\text{-}13)$$

So, from equation (2-5) or (2-6)

$$y_k = w_k \circledast x_k e_k = \sum_{m=0}^{M-1} w(m) e^{-2\pi i \frac{f_h}{f_s}(m+k\frac{M}{4})} \; x(m+k\tfrac{M}{4})$$

$$y_k = e^{-ik(\frac{f_h}{f_s}\frac{M\pi}{2})} \sum_{m=0}^{M-1} w(m) e^{-2\pi i (\frac{f_h}{f_s})m} \; x(m+k\tfrac{M}{4}) \qquad (2\text{-}14)$$

where $\frac{M}{4}$ is the decimation factor, corresponding to a 4:1 redundancy in the weighting of the time series $x_1(t)$, $x_2(t)$ by the Hanning weight coefficients given by

$$w(m) = \frac{1}{2}(1 - \cos\frac{2\pi m}{M}), \; m=0,1,\ldots,M-1.$$

To determine the frequency response of the heterodyned and low-passed time series x(t), let

$$w(t) = \frac{1}{2}(1 + \cos\frac{2\pi t}{T}) \text{ for } -T/2 \le t \le T/2$$

let

$$e(t) = e^{-2\pi i f_h t}$$

and let $x(t) = e^{2\pi i f t}$. Then from Figure 4 we have:

$$y(t) = \frac{1}{2}\int_{-T/2}^{T/2} (1 + \cos\frac{2\pi s}{T}) \, e^{-2\pi i f_h (t-s)} x(t-s)\,ds \qquad (2\text{-}15)$$

$$y(t) = \frac{1}{2}\int_{-T/2}^{T/2} [1 + \frac{1}{2}(e^{i\gamma s} + e^{-i\gamma s})]e^{2\pi i(f-f_h)t}\, e^{-2\pi i(f-f_h)s} ds \tag{2-16}$$

where $\gamma = \frac{2\pi}{T}$. If $\delta f = (f-f_h)$, then

$$y(t) = \frac{1}{4} e^{2\pi i(\delta f)t} \int_{-T/2}^{T/2} 2e^{-2\pi i(\delta f)s} + e^{-2\pi i(\delta f + \frac{1}{T})s} + e^{-2\pi i(\delta f - \frac{1}{T})s} ds \tag{2-17}$$

In discrete form (2-17) becomes:

$$4e^{-2\pi i(\frac{\delta f}{f_s})k} y_k = \sum_{m=-\frac{M}{2}}^{\frac{M}{2}-1} [2e^{-2\pi i(\frac{\delta f}{f_s})m} + e^{-2\pi i(\frac{\delta f}{f_s} + \frac{1}{M})m} + e^{-2\pi i(\frac{\delta f}{f_s} - \frac{1}{M})m}] \tag{2-18}$$

It can be shown that $\int_{-T/2}^{T/2} e^{-2\pi i(\frac{\delta f}{f_s})s}\, ds = \frac{\sin(\beta\pi T)}{\pi\beta}$ (2-19)

where $\beta = (\frac{\delta f}{f_s})$. Using (2-19), Eq. (2-18) can be approximated by,

$$4e^{-2\pi i\beta k} y_k = \frac{2\sin(\pi\beta M)}{\pi\beta} + \frac{\sin\pi(\beta + \frac{1}{M})M}{\pi(\beta + \frac{1}{M})} + \frac{\sin\pi(\beta - \frac{1}{M})M}{\pi(\beta - \frac{1}{M})M} \tag{2-20}$$

or

$$4e^{-2\pi i\beta k} y_k = \frac{2\sin(\pi\beta M)}{\pi\beta} - \frac{\sin(\pi\beta M)}{\pi(\beta + \frac{1}{M})} - \frac{\sin(\pi\beta M)}{\pi(\beta - \frac{1}{M})} \tag{2-21}$$

Eqivalently:

$$4e^{-2\pi i\beta k} y_k = \frac{\sin(\pi\beta M)}{\pi}\left(\frac{2}{\beta} - \frac{1}{(\beta + \frac{1}{M})} - \frac{1}{(\beta - \frac{1}{M})}\right) \tag{2-22}$$

$$4\pi e^{-2\pi i\beta k} y_k = \frac{\frac{-2}{M^2}}{\beta(\beta^2 - \frac{1}{M^2})} \sin(\pi\beta M) \tag{2-23}$$

$$2\pi e^{-2\pi i\beta k} y_k = \frac{\frac{1}{M2}}{\beta(\frac{1}{M^2} - \beta^2)} \sin(\pi\beta M) \tag{2-24}$$

Letting $r = M\beta = M(\frac{f-f_h}{f_s})$ in (2-24) we get:

$$2\pi e^{-2\pi i\beta k}\, y_k = \frac{M}{r(1-r^2)} \sin(\pi r)$$

or

$$\frac{2e}{M}^{-2\pi i\beta k}\, y_k = \frac{\sin(\pi r)}{\pi r(1-r^2)} = \frac{-\sin[\pi(r-1)]}{\pi r(1-r^2)} \qquad (2\text{-}25)$$

The right-hand ride of equation (2-25) is the frequency response Y(r) of the time series y_k

Clearly $Y(0) = 1$, $Y(.5) = \frac{8}{3\pi}$, $Y(1) = .5$.

So for $r = 1 = \frac{M(f-f_h)}{f_s}$ we have,

at 6-dB down, the 6-dB bandwidth

$$\frac{B}{2} = (f-f_h) = \frac{f_s}{M}$$

or

$$B_{6\text{-}dB} = \frac{2f_s}{M} \qquad (2\text{-}26)$$

The block diagram describing the implementation of the two dimensional search algorithm is shown in Figure 5. It is a continuation of part (A) of the one shown in Figure 2, in the first part of the report.

As shown in Figure 5, the double buffer containing the digitized time series $x_1(t)$ and $x_2(t)$ is demultiplexed by the software into two channels $x_1(t)$, $x_2(t)$ representing the received signal $s(t)$ at the two sensors, of respective frequencies f_o and $f_o(1+\dot{\tau})$, where $\dot{\tau}$ is the doppler shift to be estimated. The two time sequences $x_1(t)$, $x_2(t)$ are then heterodyned. The effect of the heterodyning is to select the spectral window of interest around some center frequency f_h. The width of this spectral window is approximately given by equation (2-26). As a result of the low-pass filtering and heterodyning, the output complex time sequences $y_1(t)$, $y_2(t)$ have respective frequencies $(f_o - f_h)$ and $(f_o + f_o\dot{\tau} - f_h)$. At this point $y_1(t)$, $y_2(t)$ are the input channels to the crosscorrelator that will estimate $\tau(t)$ and $\dot{\tau}(t)$.

Let N = number of complex points to be processed by the crosscorrelator. (=size of $y_1(t)$, $y_2(t)$).

Let M = number of Hanning weight coefficients.

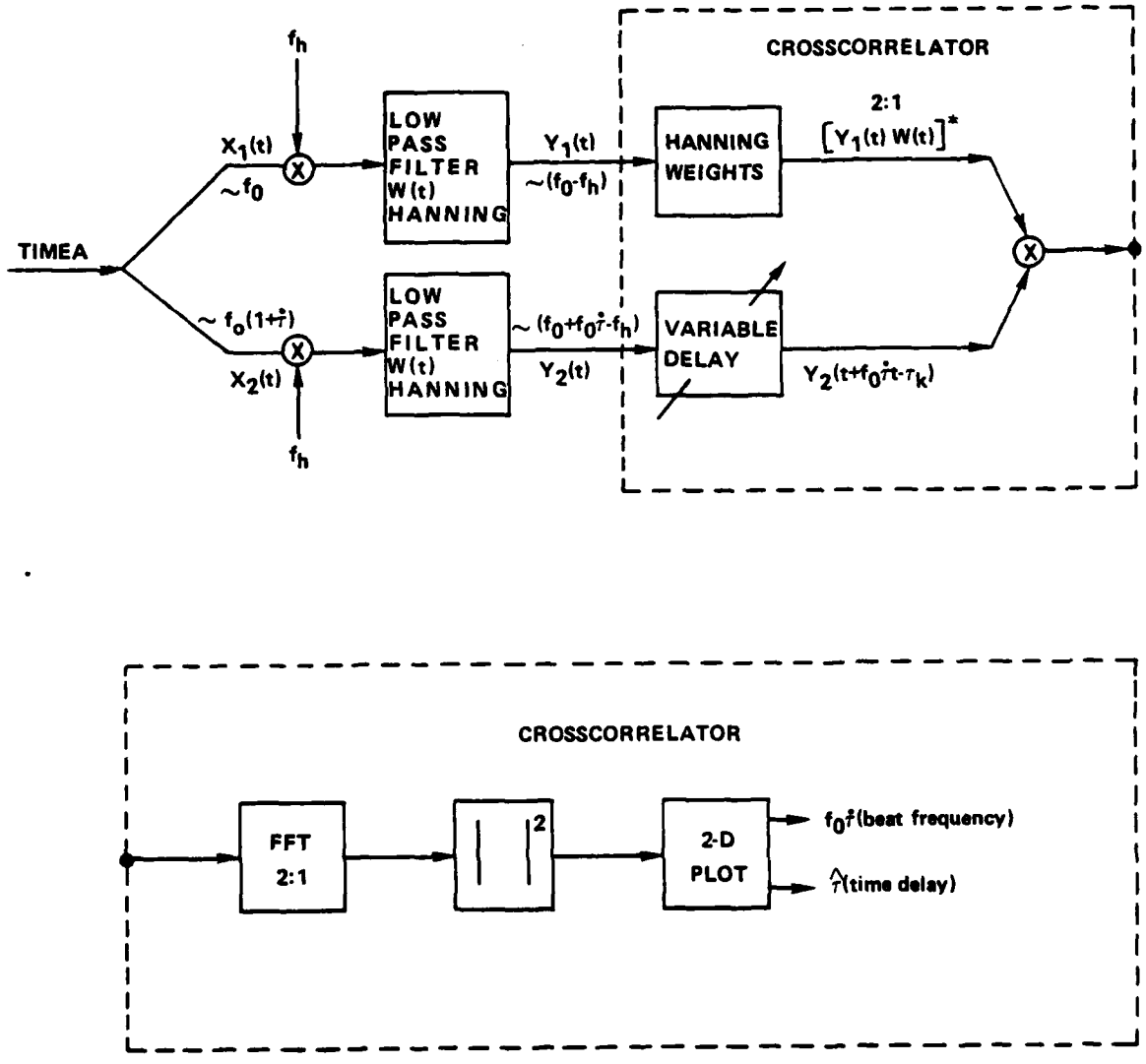

FIGURE 5 BLOCK DIAGRAM OF THE TIME DELAY AND TIME DELAY RATE ESTIMATOR

Because of the 4:1 redundancy (M/4 decimation factor in the convolution, Eq. (2-14)) in the weighting of the time sines $x_1(t)$, $x_2(t)$, we must have MN/4 points for each $x_1(t)$, $x_2(t)$. If f_s is the sampling frequency, then

$$\Delta t = \frac{\frac{MN}{4}}{f_s}$$

gives the number of seconds corresponding to the complex time series $y_1(t)$, $y_2(t)$ entering the crosscorrelator. The number of points FFT'd is $N'_{FFT} = 2N$ (we have a 2:1 redundancy in the FFT). Typical values for the parameters defined above are: M = 128 pts, N = 64 pts, f_s = 1024 pts/sec. These values for equation (2-26), give

$$B = \frac{2f_s}{M} = 16\text{Hz}$$

frequency window to be crosscorrelated. Furthermore the duration Δt of the time cuts (size of $y_1(t)$, $y_2(t)$) entering the crosscorrelator is,

$$\Delta t = \frac{\frac{MN}{4}}{f_s} = \frac{(32)\ (64)}{1024} = 2 \text{ seconds.}$$

Moreover, the FFT sampling frequency, (decimated frequency), f_{SFFT}, is

$$f_{SFFT} = \frac{N}{\Delta t} = \frac{64}{2} = 32\text{pts/sec},$$

per channel. Therefore the FFT time,

$$T_{FFT} = \frac{N'FFT}{f_{SFFT}} = \frac{2N}{\frac{N}{\Delta t}} = 2\Delta t = 4 \text{ seconds}$$

because of the 2:1 redundancy in the FFT. The FFT resolution is

$$R_{FFT} = \frac{1}{T_{FFT}} = \frac{1}{2\Delta t} \text{ Hz/bin.}$$

Figure 6 shows how the 2:1 redundancy in the FFT and the variable delay scheme are implemented in the MAP-300 array processor. For this algorithm we have chosen a slow time delay search (through shifting in the time domain) and a fast time delay rate search (via an FFT).

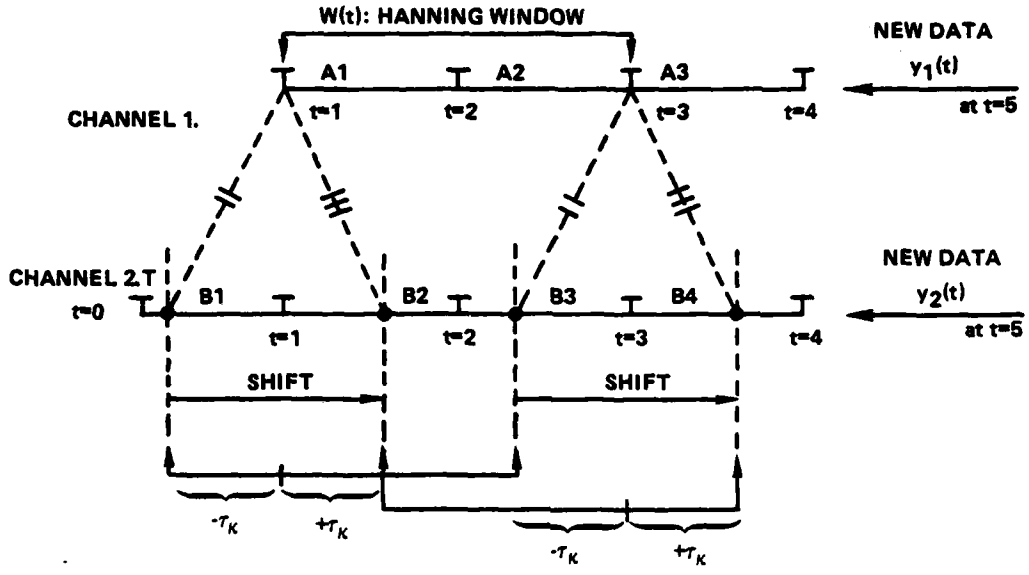

FIGURE 6 VARIABLE TIME DELAY SCHEME AND 50% OVERLAP

IN THE WEIGHTING OF CHANNEL 1

Segments A1 through A3 and B1 through B4, each contain the N points entering the crosscorrelator. The variable t represents units of time. In this case each unit of time is of duration Δt seconds. For the values considered previously, N=64 pts and Δt = 2 seconds. Before any new data is received, segments A1 and A2 are weighted with a 2N-point Hanning weight. The resulting vector of size 2N is V_1. For channel 2, to accomodate for a delay window of $\pm\ \tau(t)$ seconds, we pick the vector V_2, which starts τ_k points to the left of $\underline{t}$ = 1, where

$$\tau_k = \frac{N\tau(t)}{\Delta t} \text{ pts.}$$

We then form the point-by-point vector product $U = V_1^* V_2$, which is FFT'd. Following this we form a new vector V_2 of length 2N points, starting at (τ_k -1) points to the left of t = 1 and again we form a new U vector which is again FFT'd. This procedure is repeated ($2\tau_k$ + 1) times so that we sweep through all points representing the negative and positive delay window. Once

the delay search is completed for this fixed time cut of duration Δt seconds, we shift the segments A2→A1, A3→A2, B2→B1, B3→B2, B4→B3 and the newest segment of data for $y_1(1)$, $y_2(t)$ enters in A3 and B4 respectively, in such a way that the data points are ordered in time. Moreover, the units of time are also updated by 1. The delay search is then repeated for the new time cut. This procedure enables us to search for $\tau(t)$ within a $\pm\Delta t = \pm 2$ second window.

So for every time cut and for every delay point τ_k, after $y_1(t)$ has been Hanning weighted in a 2:1 fashion, conjucated and multiplied by a delayed $y_2(t)$, we take the FFT and calculate the power spectrum of the product. We then search for the location of the peak in the power spectrum, from which we can get an estimate of the delay rate $\dot{\tau}$ (see below). With an appropriate shifting of the power spectrum the zero delay rate ($\dot{\tau} = 0$) corresponds to the frequency bin in the middle of the power spectrum. This enables us to look only at a window centered at the middle of the power spectrum. The width of the window can vary as a function of the $\dot{\tau}$ that is to be estimated.

The change $\Delta\tau$ in the delay τ, per update of duration Δt, is given by

$$\Delta\tau = (\Delta t)\dot{\tau} = \frac{1}{2} T_{SFFT}\dot{\tau} = \frac{1}{2}\frac{2N}{f_{SFFT}}\dot{\tau} = \frac{N}{f_{SFFT}}\dot{\tau}$$

where $\dot{\tau}$ is the delay rate. The frequency cell where the peak in the power spectrum shows up for every time cut (update) and for every delay point τ_k is given by,

$$n_{FFT} = f_o\dot{\tau}\, T_{FFT} \doteq f_h\dot{\tau}\quad T_{FFT} = f_h\dot{\tau}\,\frac{2N}{f_{SFFT}} \tag{2-27}$$

The position of the peak at the $(\tau_k)^{th}$ delay point is

$$n_{\tau_k} = f_{SFFT}\,\tau$$

So for f_{SFFT} = 32pts/sec and τ = 1/16 sec,

$$n_{\tau_k} = 2$$

positions from the zero delay position.

The rate $\Delta_{n_{\tau_k}}$ at which the position of the peak in the power spectrum is moving for every update Δt is

$$\Delta n_{\tau_k} = \frac{1}{2} N'_{FFT}\,\dot{\tau} = \frac{1}{2}(2N)\,\dot{\tau} = N\dot{\tau} \tag{2-28}$$

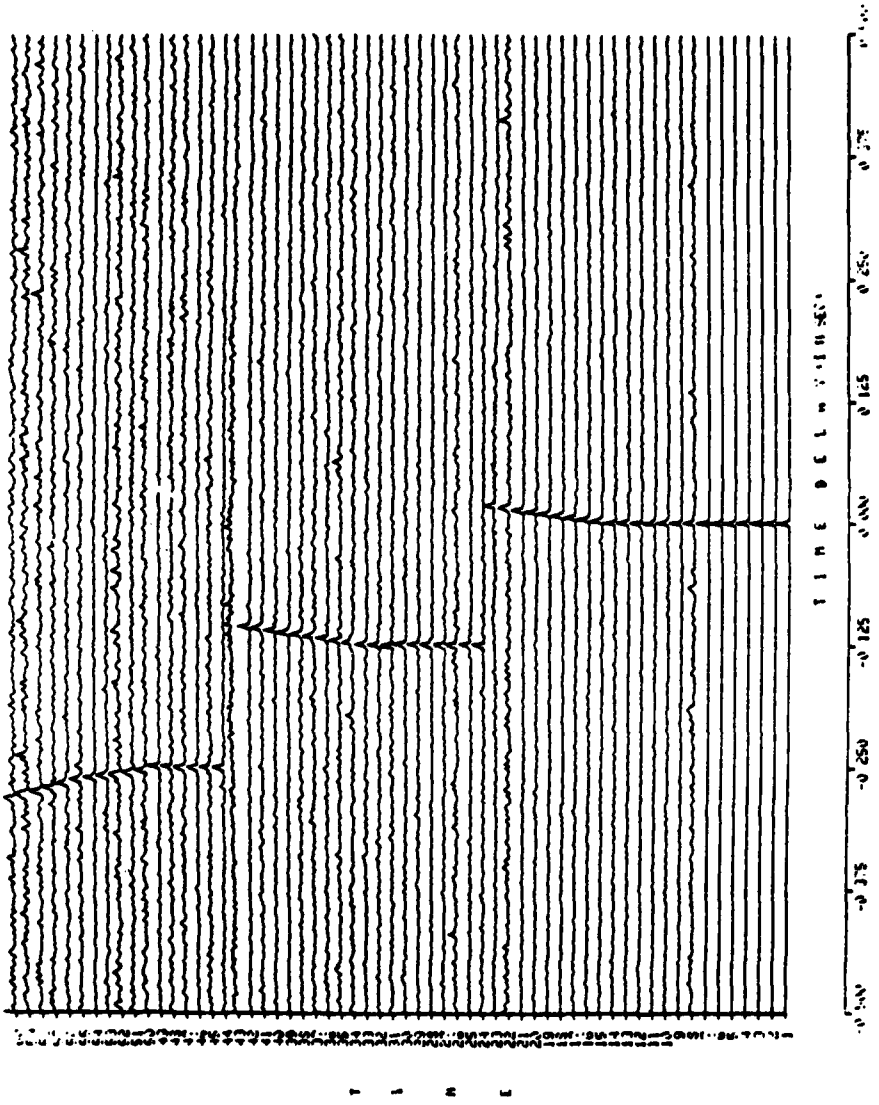

FIGURE 7 CORRELOGRAMS OF A WHITE NOISE SIGNAL. DIFFERENT DELAYS AND DELAY RATES ARE ILLUSTRATED

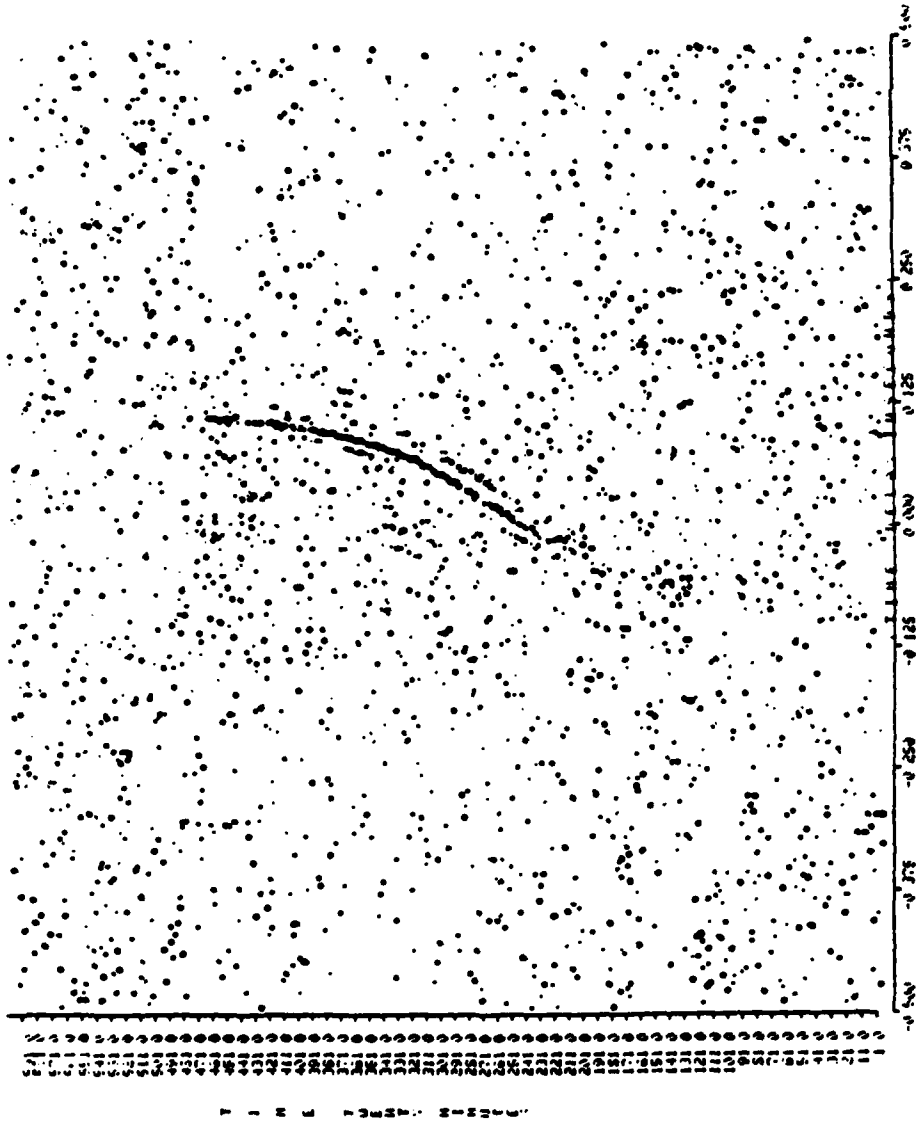

FIGURE 8 TIME DELAY ESTIMATION WITH NO DOPPLER COMPENSATION
FOUR STRONGEST PEAKS IN CORRELOGRAM
TWO SECOND POST-INTEGRATED CORRELOGRAMS
CROSS CORRELATION WINDOW OF WIDTH 256 Hz

So from (2-27)

$$\Delta_{n_{\tau_k}} = N\dot{\tau} = N\frac{f_{SFFT}}{2Nf_h}n_{FFT} = \frac{1}{2}\left(\frac{F_{SFFT}}{f_h}\right)n_{FFT}$$

where f_h is the heterodyne frequency.

ILLUSTRATION OF RESULTS

The figures that follow illustrate some results obtained using the algorithms described in this report. In all the figures the locations of three or four strongest peaks in the correlogram were plotted by the host computer.

Figure 8 shows the time delay track of a signal emanating from a target of interest. This track was obtained using the one dimensional sheme with no doppler compensation. The spacing between the sensors is approximately 250 yards. We estimated that the target's speed is about 6 knots and that the target is located at about 2600 feet from one of the sensors at the CPA time to this sensor. We processed, for 20 minutes, a spectral window of width 256 Hz.

The scenario for the time delay tracks shown in Figures 10 and 11 is shown in figure 9.

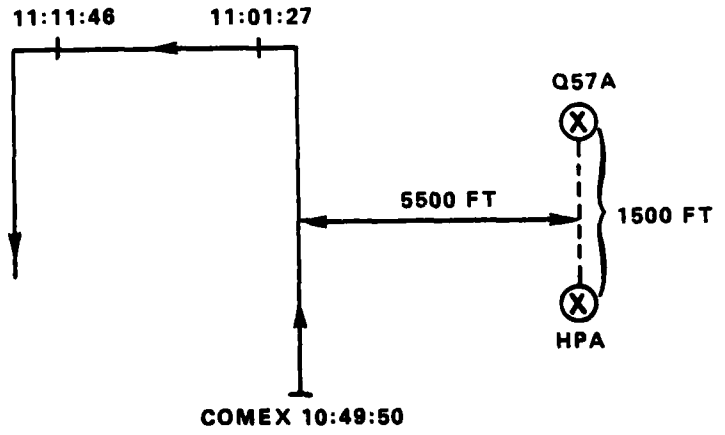

FIGURE 9 SCENARIO FOR FIGURES 10 AND 11

The target is a towed sound source radiating broadband energy from 200 to 1000 Hz. It is moving at a speed of 6 knots.

Figure 10 shows the time delay track between a Q57A buoy and a sensor on a Horizontal Planar Array. The distance between them is approximately 1500 feet. It is a 30 minute run, the correlograms are averaged and plotted every 4 seconds

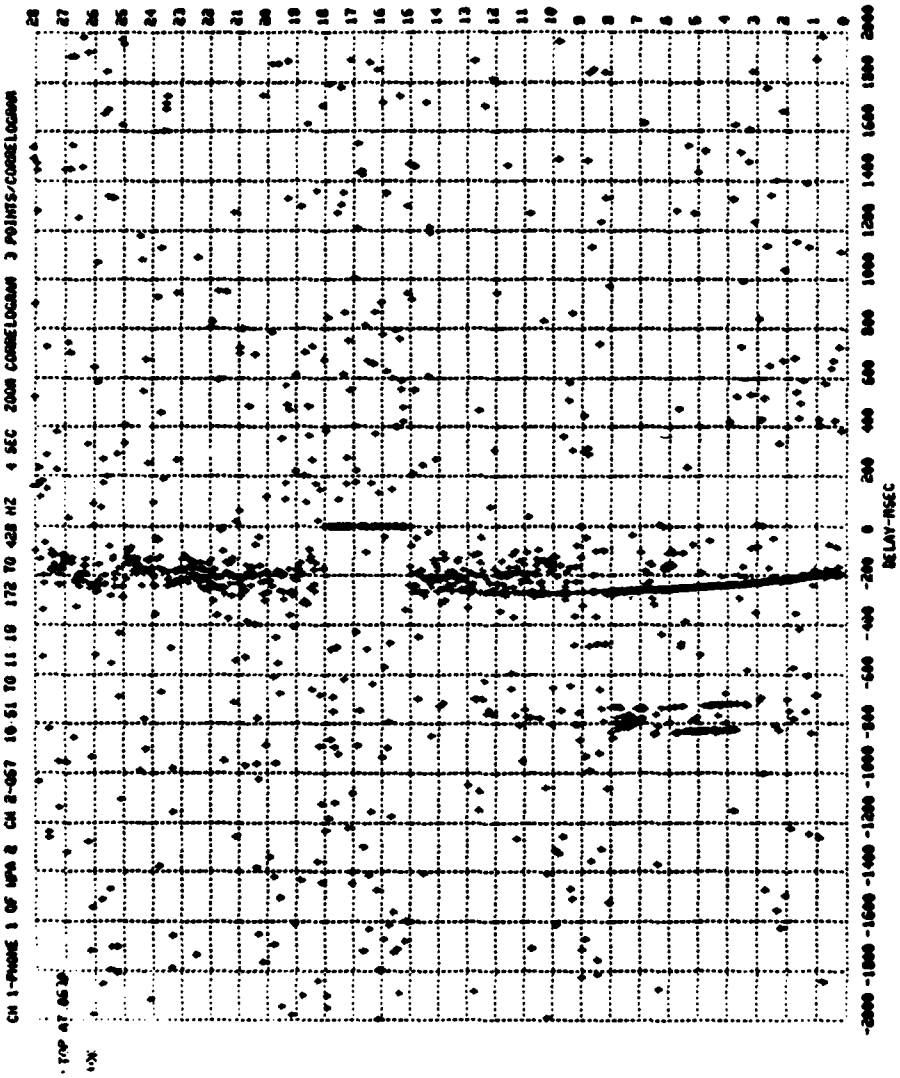

Figure 10 Time delay track between a Q57A buoy and a sensor on a HPA
Three strongest peaks in correlogram
Four second post-integrated correlograms
Cross correlation window 172 to 428 Hz

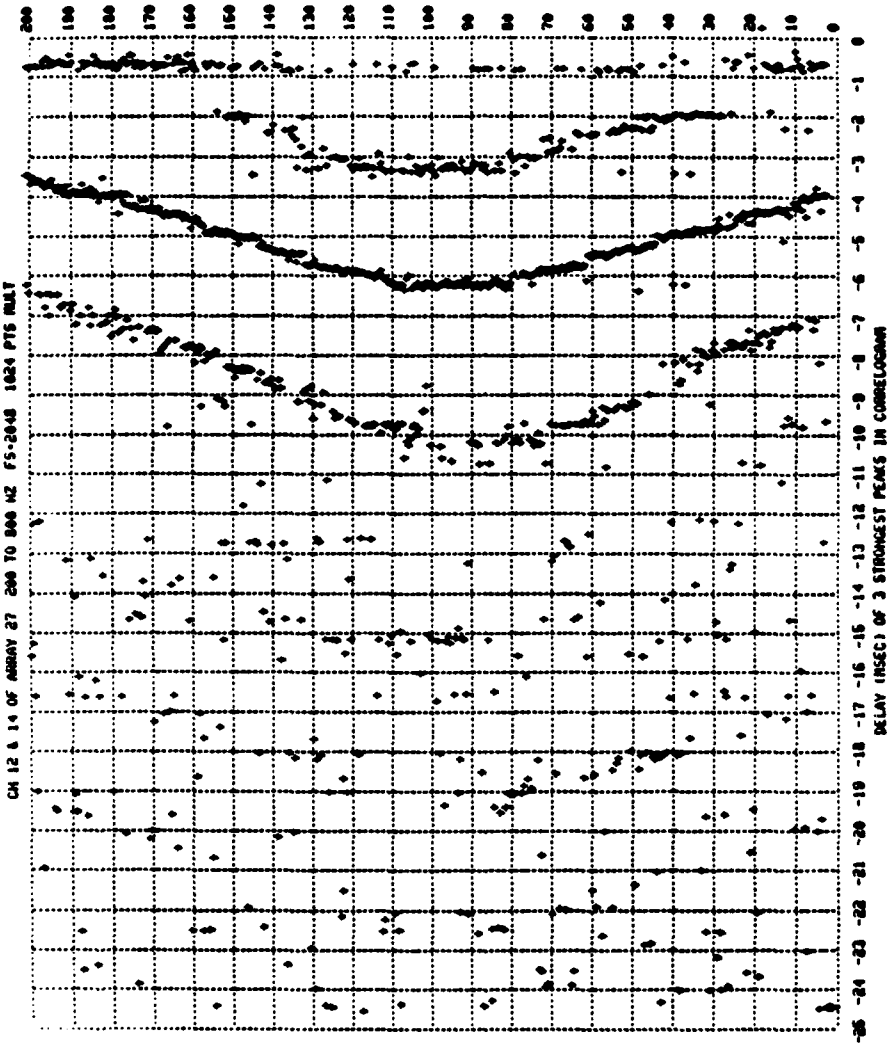

Figure 11 Time delay track between two sensors on a HPA
Three strongest peaks in correlogram
Cross correlation window 200 to 800 Hz

and the three largest peaks are plotted. For the first 10 minutes a direct signal from the target is received and after the turn, for the remaining 20 minutes the bottom bounce signals are received.

Figure 11 shows the time delay track of the signal from the target of Figure 9, received at two sensors located on a Horizontal Planar Array.

The two dimensional search algorithm was used for the scenario depicted in Figure 12.

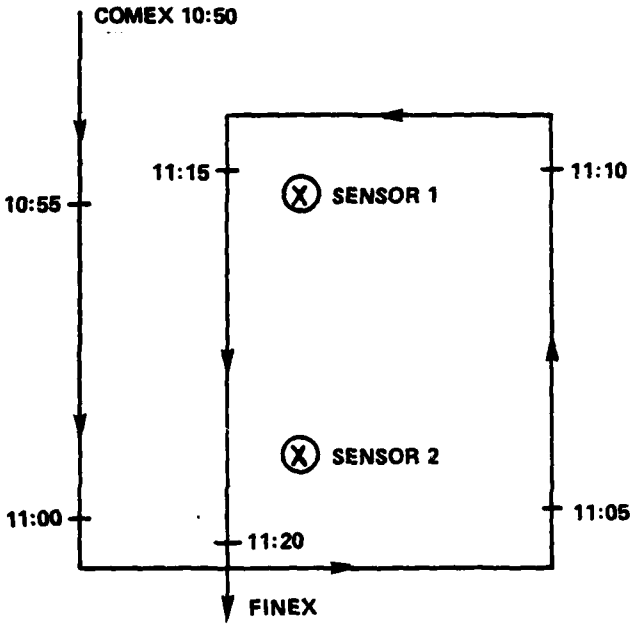

FIGURE 12 SCENARIO FOR FIGURES 13 AND 14

The spacing between the sensors is approximately 2200 yards and the target is moving at a speed of about 15 knots.

The algorithm was successful only when we processed frequency windows below 40Hz. Figure 13 and 14 show the time delay track and the change in time delay for 30 minutes. For both cases we sampled at fs = 512 pts/sec, and the decimated frequency was 16 Hz (16 pts/sec out of the heterodyne and low-pass filter). We crosscorrelated 16 seconds of data and plotted the correlograms every 8 seconds. The time delay window was $\pm$2 seconds. In Figure 13 we processed a window of 8Hz centered at 16Hz and in Figure 14 the same frequency window was centered at 30Hz. As we increased the heterodyne frequency, the time delay track dissappeared.

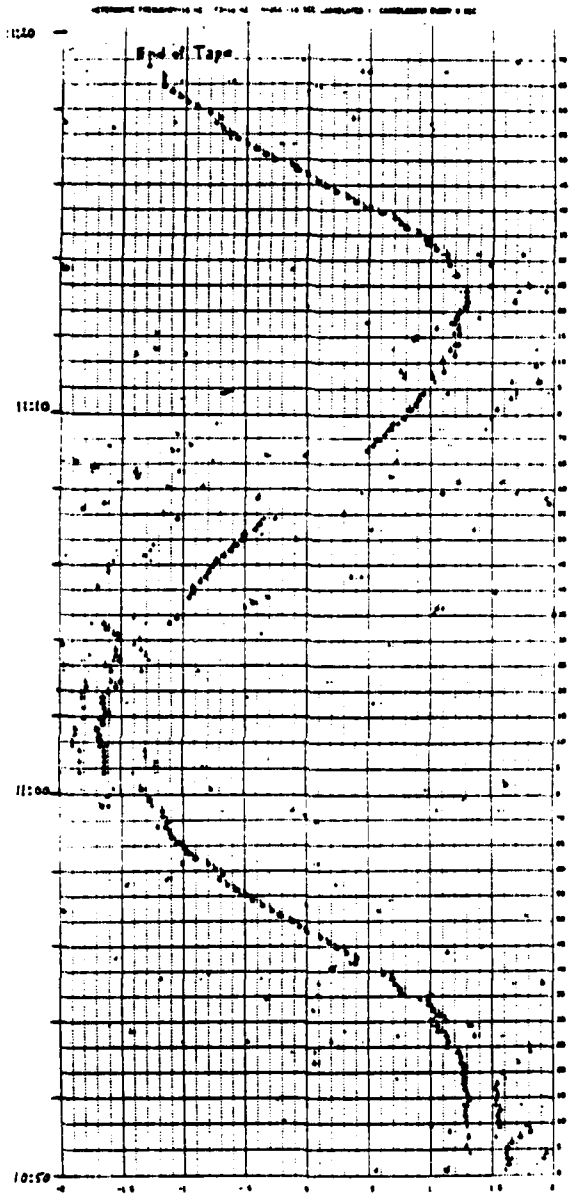

Figure 13 Time delay track with doppler shift compensation
Heterodyne frequency: 16 Hz
Decimated frequency: 16 Hz
Correlograms every 8 seconds
16 second of data were cross correlated

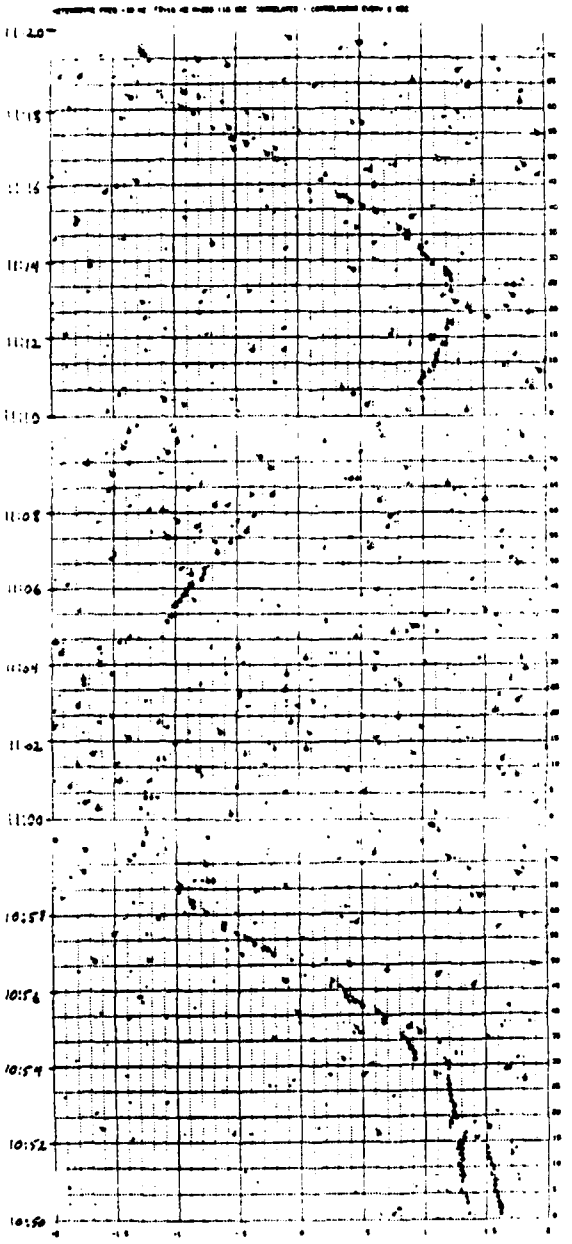

Figure 14 Time delay track with doppler shift compensation
Heterodyne frequency: 30 Hz
Decimated frequency 16 Hz
Correlogram every 8 seconds
16 seconds of data were cross correlated

SUMMARY OF RESULTS

For closely spaced sensors and slow, non-maneuvering targets the algorithm described in the first part of the report can be used. In all other cases, when doppler compensation is necessary, the two dimensional search routine can be used, although its success is limited to processing broadband energy at the very low end of the spectrum.

DISTRIBUTION

	Copies
ASW Systems Project Office Attn: R. Delaney (ASW-138) LCDR G. Watson Washington, DC 20360	 1 1
Commander Naval Air Systems Command Department of the Navy Attn: CDR J. Hagy (PMA-264) Washington, DC 20361	 1
Commanding Officer Naval Air Development Center Attn: Dr. B. Steinberg M. Higgins Warminster, PA 18974	 1 1
Commanding Officer Naval Intelligence Support Center 4301 Suitland Road Attn: AWC D. Christofferson (NISC 23) Washington, DC 20390	 1
Commander Naval Underwater Systems Center Attn: G. Mayer New London, CT 06320	 1
Tracor, Inc. 6500 Tracor Lane Attn: F. Weidman Austin, TX 78721	 1
Office of Naval Research 800 N. Quincy St. Attn: Code 715 Arlington, VA 22217	 2
Defense Technical Information Center Cameron Station Alexandria, VA 22314	 12


DAT
ILM